

CO adsorption on Fe_N ($N = 1-4$) transition metal clusters: a density functional theory study

Vivek Sinha and Pradip Kr. Ghorai*

Department of Chemical Sciences, Indian Institute of Science Education and Research, Kolkata 741 252, India

The structures and stabilities of the $\text{Fe}_N(\text{CO})_m$ ($N = 1-4$, $m = 1-5$) clusters have been theoretically studied at the density functional theory (DFT) and *ab initio* levels of theory. In particular, the energetic, structural and vibrational frequencies of carbon monoxide (CO) chemisorptions on iron clusters are studied and compared with those of nitric oxide (NO) and ammonia (NH_3) adsorption. While the C–O and N–O bond lengths and vibrational frequencies strongly depend on cluster size and ligand population, the N–H bond length and vibrational frequency are independent on both cluster size and ligand population. For a particular Fe_N cluster, the vibrational frequency increases as the ligand population increases. On the other hand, keeping the number of ligands fixed, the vibrational frequency decreases significantly with the Fe_N cluster size. NO and CO being strong field ligands in the spectrochemical series, we have seen red shift of the vibrational frequencies with both cluster size and ligand population. As NH_3 is a weak field ligand, we do not observe any variation. We have also observed that the HOMO–LUMO gap of both $\text{Fe}_N(\text{CO})_m$ and $\text{Fe}_N(\text{NO})_m$ clusters strongly depends on N and m . For $\text{Fe}_N(\text{NH}_3)_m$ cluster, HOMO–LUMO gap decreases as more NH_3 molecules are adsorbed on the metal centre.

Keywords: Adsorption, density functional theory, metal cluster, vibrational frequency.

Introduction

THE connecting link between molecular physics and condensed matter is the different type of atomic structures. Hence study of different metal clusters may be important to understand the properties evolving from nanoscopic regions to bulk. It is known that change in dimensionality from volume to surface to wires to molecules exhibits many unconventional properties¹. The finite size effects not only distinguish a cluster from bulk materials but also strongly influence the magnetic, optical and electronic properties of a material. These properties are neither found in the atomic state of these metals nor can be found

in the extended solid-like crystals. Moreover, clusters of transition metals (TM) have been studied using experimental methods for a relatively long time². These experiments usually do not give any direct insights into structures of the observed clusters and hence cannot explain many properties. For example, the experiment cannot explain the size-dependent magnetic properties of iron clusters.

The adsorption of carbon monoxide (CO) to TM clusters has been studied extensively because it exists as an important mechanistic step in the chemical pathway of many catalytic reactions³⁻⁵. Nikolaev *et al.*⁶ developed a high-temperature, high-pressure experimental procedure to form iron clusters which catalyse the growth of single-walled carbon nanotubes in the presence of CO flow. Hence theoretical studies of CO adsorption on TM clusters are of significant importance. Though there are large numbers of experimental and theoretical studies of bare iron clusters available in the literature⁷⁻¹¹, a complete trend for the structural and electronic properties of CO adsorption on iron clusters has not been studied in detail. Towards molecular-level understanding of the adsorption properties of CO on iron clusters, it is necessary for a theoretical study of ligand adsorption on iron clusters. Zeinalipour-Yazdi *et al.*³ studied the trends for single CO chemisorption on TM clusters. They observed an increase of the electronic *d*-shell occupancy and the principle quantum number (n) in TM clusters. Here we increase the number of CO molecules adsorbed on the Fe_N ($N = 1$ to 4) clusters. As the C–O bond strength is sensitive to the binding site of metals, the C–O metal systems are a useful model to characterize the binding site at metal centres. The adsorption of two other ligands, namely NO and NH_3 on iron clusters has also been studied and their adsorption characteristics have been compared with CO.

Computational details

The minimum energy configurations of bare Fe_N clusters for singlet spin state are obtained by optimizing the spin multiplicity $S = 0$ state geometries. The structures are optimized without any symmetry constraints. For each cluster, the local minima of the potential energy surface

*For correspondence. (e-mail: pradip@iiserkol.ac.in)

are confirmed by the harmonic vibrational frequency without imaginary mode. By taking this optimized Fe_N clusters, again we optimize the $Fe_N(CO)_m$ systems to study the adsorption properties of CO on iron clusters. In all calculations, the convergence thresholds are set to 0.000015 Hartree/Bohr for the forces, 0.00006 Å for the displacement and 10^{-6} Hartree for the energy change. All calculations are performed with the density functional theory (DFT) with unrestricted Becke's three-parameter hybrid exchange functional¹² combined with Lee–Yang–Parr non-local correlation function¹³, abbreviated as B3LYP. We have used LanL2DZ basis set^{14,15} along with the corresponding Los Alamos relativistic effective core potentials¹⁶ provided by Gaussian 03 package¹⁷. For NO and NH_3 adsorption, we followed similar methods as discussed above for CO adsorption.

Results and discussion

Structures and stability of bare Fe_N clusters

First we present the singlet-state structures of bare Fe_N clusters and the structures of CO adsorbed on these Fe_N clusters. The minimum energy structures and their corresponding energies for $S = 0$ state are shown in Figure 1. Fe–Fe distance increases with the cluster size. Fe–Fe distance for $N = 2$ is 1.72 Å, whereas it is 2.08 and 2.32 Å for $N = 3$ and 4 respectively. A similar trend was found in earlier studies also^{7,8}. While Fe_3 adopted a triangular geometry, Fe_4 is found stable in a butterfly shape. The stability of the Fe_N singlet-state clusters are discussed in terms of atomic averaged binding energies (E_b) and energy gap between the highest occupied molecular orbital (HOMO)

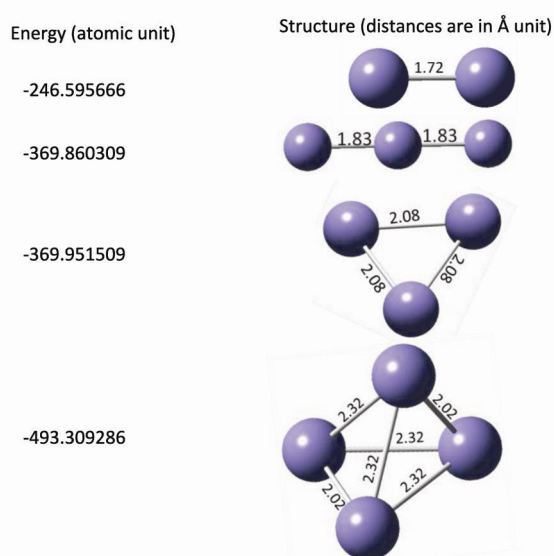


Figure 1. Optimized structures and energies of bare Fe_N clusters for $S = 0$ state.

and lowest unoccupied molecular orbital (LUMO). We have calculated E_b for the bare Fe_N cluster by using the following formula

$$E_b = [NE(Fe) - E(Fe_N)]/N, \quad (1)$$

where $E(*)$ represents the energies of the Fe atom and Fe_N clusters. Figure 2 shows that E_b increases monotonically with the total number of Fe atoms in the bare Fe_N clusters. For $N = 2-4$, E_b increases quickly from 1.15 eV/atom for the dimer to 2.025 eV/atom for the tetramer, which corresponds to the structural transition from two to three dimensions. We have also observed that the Fe_N clusters are more stable than Mn_N metal clusters¹⁸.

Structures and stability of $Fe_N(CO)_m$ cluster

Figure 3 shows the optimized $Fe(CO)_m$ ($m = 1-5$) structures. The different parameters related to these structures are discussed below. Figure 4 shows the variation of Fe–C bond length as a function of cluster size and ligand population. We separately discuss the different structures and stability of $Fe_N(CO)_m$ clusters.

(i) For $N = 1$, the Fe–C bond length varies monotonically as number of CO molecule adsorbed on the metal centre. For $m = 1-3$, the Fe–C bond length increases as more CO molecules are adsorbed. For $m = 4$ and 5, due to carbon–carbon interaction (see Figure 4) the average Fe–C bond length slightly decreases.

(ii) For $N = 2$, there are two different types of CO adsorption – (a) terminal adsorption: when carbon is bonded with one Fe atom and (b) bridging adsorption: when one carbon atom is bonded with two Fe atoms. The bridging Fe–C distance is more compared to terminal Fe–C distance. This is due to weaker Fe and C interaction when one carbon atom bridges with two iron atoms. Fe–C bond distance increases as more CO molecules are adsorbed on the clusters.

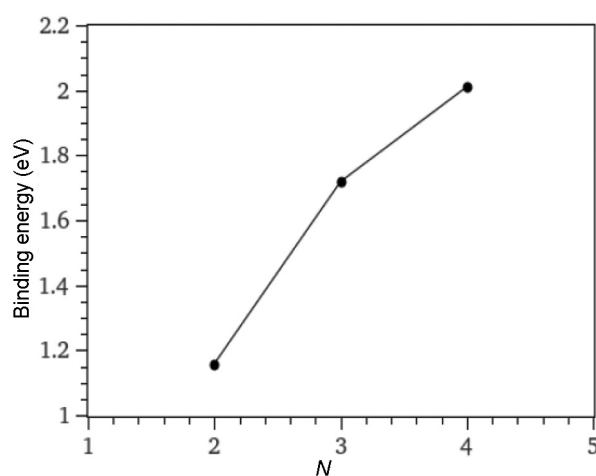


Figure 2. Binding energy for bare Fe_N clusters.

(iii) For $N=3$, we observe similar behaviour (as with $N=2$) for both terminal and bridging adsorption of CO molecule. The Fe–C bond distance for terminal adsorption increases with CO adsorption, but for bridging adsorption the Fe–C bond distance varies nonmonotonically. For $m=1$ and 2, though there is only one bridging adsorption of CO, the Fe–C distance decreases due to terminal adsorption of CO molecule. This indicates that the Fe–C bond distance not only depends on the size of the metal cluster and the ligand concentration, but also on how (terminal or bridging) the ligand adsorbs on a metal centre.

(iv) For $N=4$, we have studied the adsorption of CO up to $m=6$. As the CO adsorption per Fe atom is less for the bigger metal cluster, we do not observe any change in Fe–C bond distance.

For all the Fe_N clusters, the Fe–Fe distance also varies with CO adsorption compared to bare Fe_N clusters.

C–O bond length, vibrational frequency and adsorption energy

The catalytic activity can be evaluated by the bond length and vibrational frequency of small molecules adsorbing on the metal cluster. The C–O bond lengths and vibrational frequencies are shown in Figure 5 *a* and *b* respectively. The C–O bond length is more for the large Fe_N cluster. When only one CO molecule adsorbs on the metal centre, the C–O bond length is 1.185 Å for Fe_1 , whereas for Fe_2 , Fe_3 and Fe_4 clusters it is 1.19, 1.23 and 1.31 Å respectively. Interestingly, when more CO molecules are adsorbed, the C–O bond length for Fe_1 decreases slowly, whereas for bigger clusters (Fe_2 , Fe_3 and Fe_4) the bond length decreases significantly. As the cluster size increases, the C–O bond activation is more on account of higher electron density which comes from the metal centre. Within a given cluster, as the ligand population increases, the charge transfer to individual carbon

atom of CO is reduced and hence the increase in C–O bond length is suppressed.

The C–O vibrational frequencies depend on the cluster size and number of ligands adsorbed on the cluster. For a particular Fe_N cluster, the vibrational frequency increases as the ligand population increases. On the other hand, keeping the number of ligands fixed, the vibrational frequency decreases significantly with cluster size. For a free CO molecule the vibrational frequency is 2028.87 cm^{-1} , whereas it is 1931.46, 1869.99, 1688.18 and 1350.09 cm^{-1} for Fe_1 , Fe_2 , Fe_3 and Fe_4 respectively. This indicates that large red shift of adsorption band occurs under the interaction of Fe atoms. As Fe–C interaction increases with the cluster size, C–O vibrational frequency decreases. Therefore, the large C–O bond lengths correspond to the low vibrational frequency. Similar trend is observed when more C–O molecules are adsorbed on the clusters. Previously this was observed by Tian *et al.*¹⁸ for Mn_N cluster. The increased antibonding $2\pi^*$ is responsible for the red shift of the C–O vibrational frequency.

The chemical activity of a cluster is often measured in terms of adsorption energy (E_{ads}), which is defined as

$$E_{ads} = E(Fe_NCO_m) - E(Fe_N) - mE(CO), \quad (2)$$

where $E(*)$ is the total energy of the Fe_N , CO and Fe_NCO_m . Figure 5 *c* shows the variation of adsorption energy as a function of ligand population for Fe_N ($N=1-4$) clusters. We observe that E_{ads} increases with increase in ligand population. Except Fe_1 , the adsorption energy decreases with ligand population. However, for Fe_3 and Fe_4 , E_{ads} decreases slowly with ligand population compared to Fe_1 and Fe_2 .

HOMO–LUMO gap of $Fe_N(CO)_m$

Figure 6 shows the variation of HOMO–LUMO gap for $Fe_N(CO)_m$ systems. One can note that the dependence of

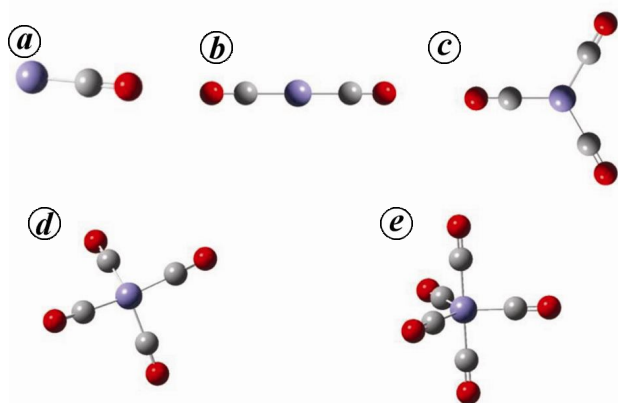


Figure 3. $Fe(CO)_m$ structures for (a) $m=1$, (b) $m=2$, (c) $m=3$, (d) $m=4$ and (e) $m=5$ respectively.

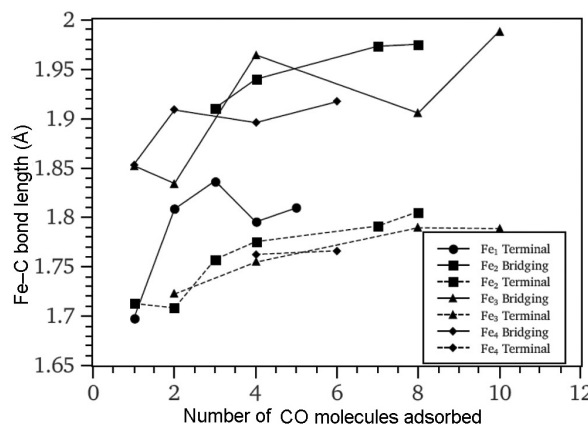


Figure 4. Variation of Fe–C bond distance for different $Fe_N(CO)_m$ clusters.

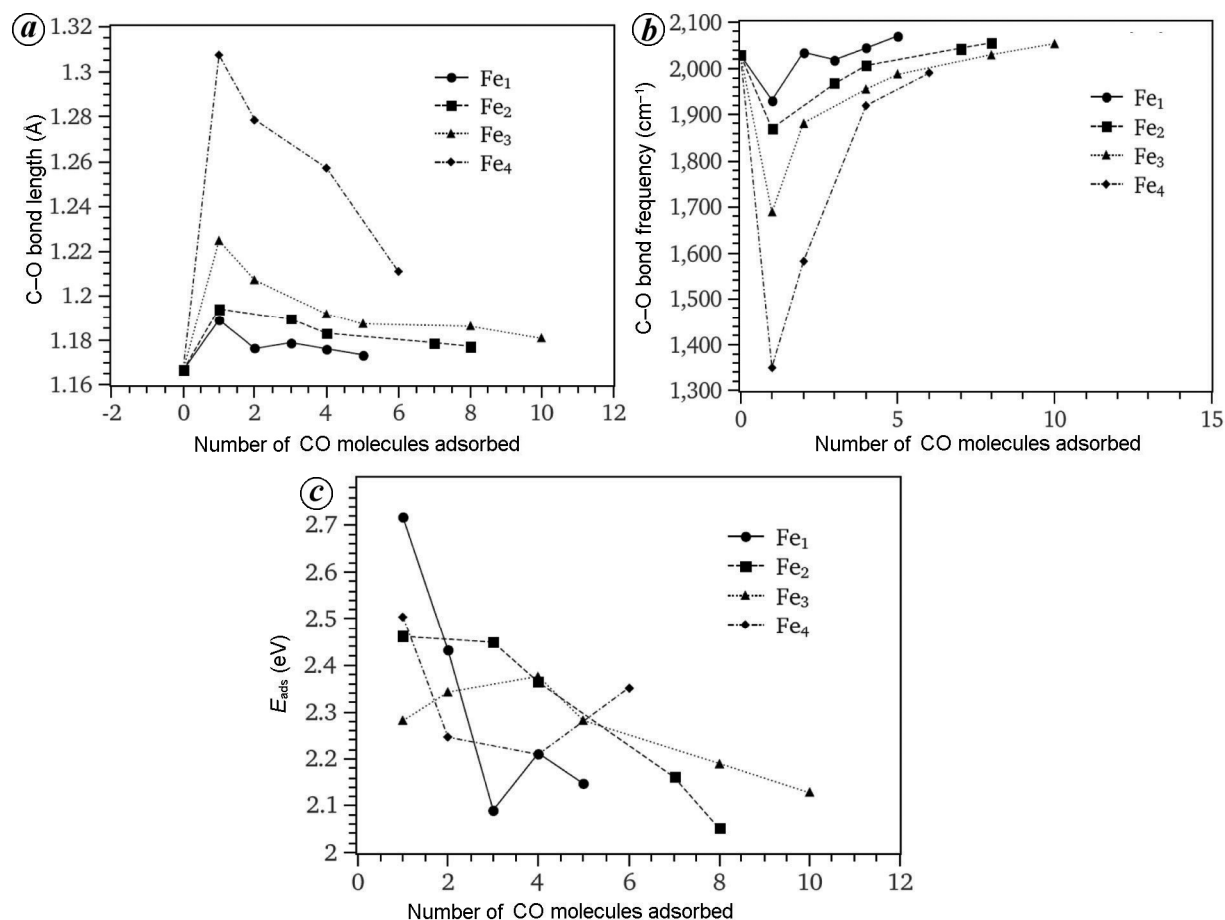


Figure 5. (a) C–O bond length and (b) vibrational frequency as a function of ligand population. (c) CO adsorption energy as a function of ligand population on different Fe_N clusters.

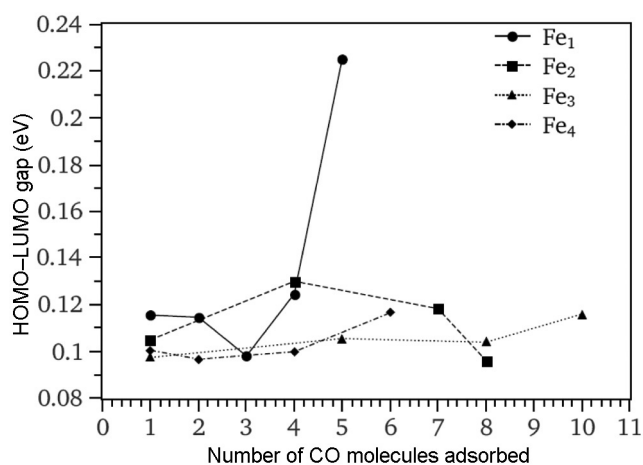


Figure 6. HOMO–LUMO gap for Fe_N(CO)_m clusters.

HOMO–LUMO gap on ligand population is different for different cluster sizes. For Fe₁(CO)_m clusters, we observe many fluctuations as the ligand population increases. For Fe₂(CO)_m clusters, initially the gap increases and then decreases. For Fe₃(CO)_m and Fe₄(CO)_m clusters, HOMO–

LUMO gap increases as more CO molecules are adsorbed on the metal centre. We find the highest HOMO–LUMO gap for Fe₁(CO)₅ system, which probably is the most stable structure among all the systems we have studied. This extra stability may be attributed to its highly symmetric pentagonal bi-pyramidal geometry.

Comparison of CO ligand properties with NO and NH₃

We know that NO is also a strong field ligand and in general NH₃ is a weak field ligand in the spectrochemical series. We would like to study how N–O, N–H bond lengths, N–O, N–H vibrational frequencies, adsorption energies and HOMO–LUMO gap depend on iron cluster size and ligand population compared to CO adsorption. Figure 7a and b shows the N–O and N–H bond variation with ligand population on Fe_N (N = 1–4) clusters. As NO is also a strong field ligand like CO, we observed similar trend (see Figure 5a). The N–O bond length is maximum for Fe₄ cluster and decreases as more NO molecules are adsorbed on the metal centre. On the other hand, as NH₃

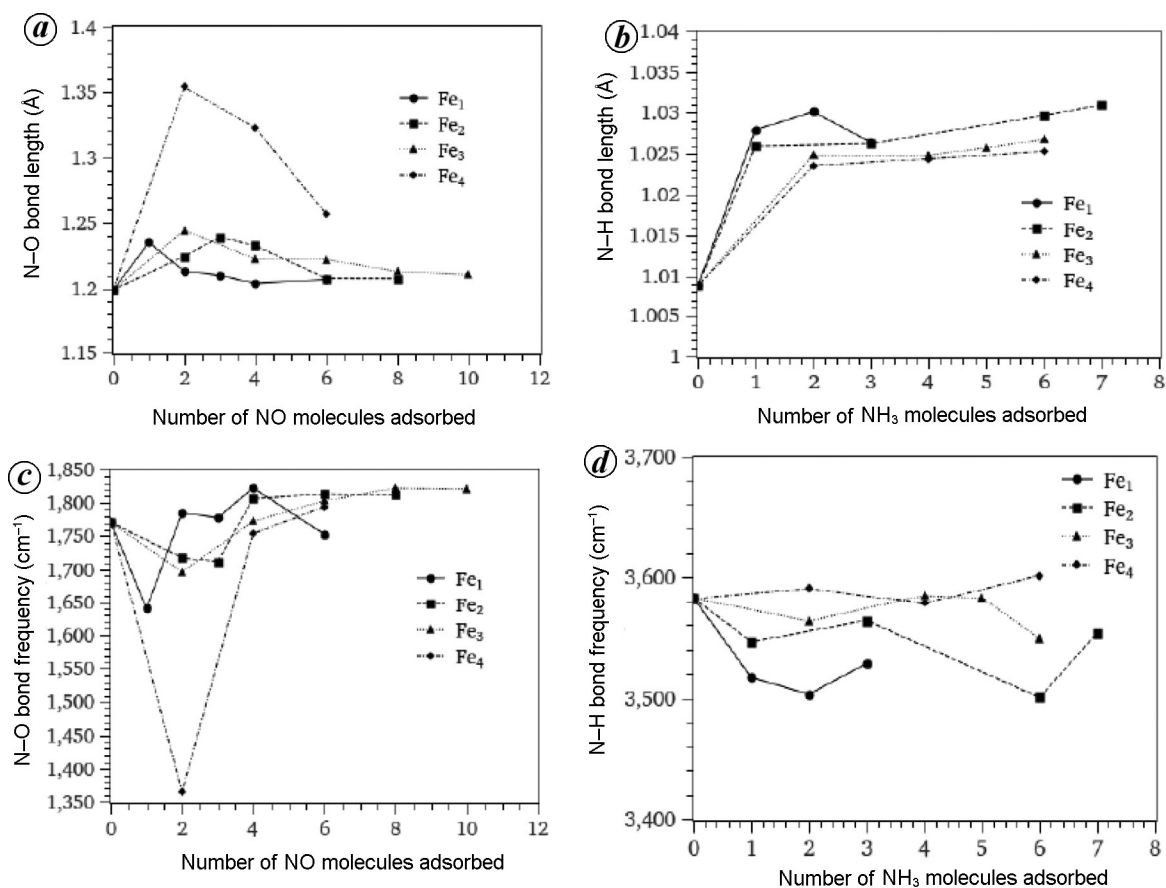


Figure 7. (a) N–O and (b) N–H bond length for NO adsorption on different Fe_N clusters as a function of ligand population. (c) N–O and (d) N–H vibrational frequency on different Fe_N clusters as a function of ligand population.

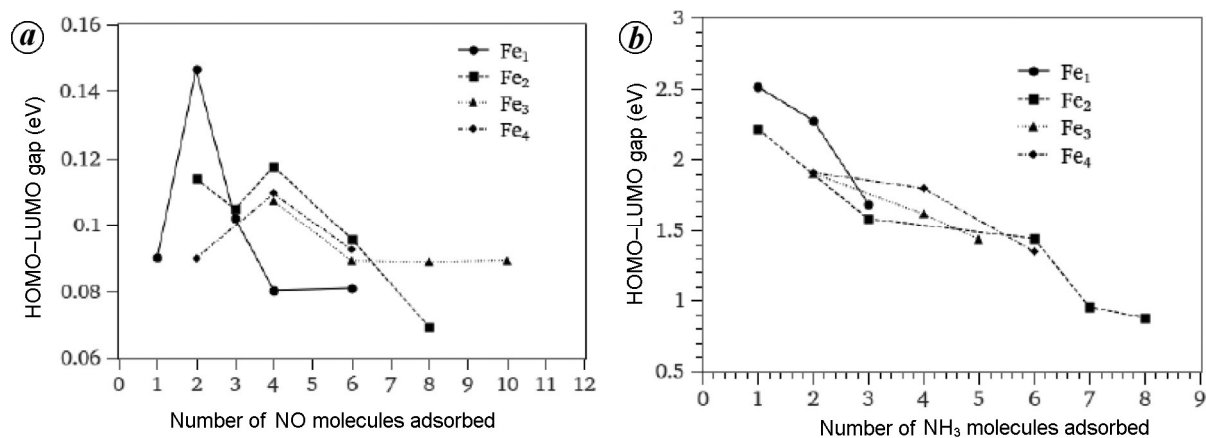


Figure 8. HOMO–LUMO gap for (a) Fe_N(NO)_m and (b) Fe_N(NH₃)_m clusters.

is a weak field ligand, the N–H bond length neither depends on the cluster size nor the ligand population. This again confirms that for the strong field ligand, i.e. for π acceptor ligands, the increasing occupancy of $2\pi^*$ orbital weakens the bond strength and hence enlarges the C–O and N–O bond lengths. Also note that NO and CO are triply-bonded species, while ammonia has N–H single

bond. This may point to some characteristic to back donation, which occurs in case of CO and NO due to the π bond.

The dependence of vibrational frequency on cluster size and ligand population for NO and NH₃ is shown in Figure 7c and d respectively. NO being a strong field ligand we observe red shift of the vibrational energy, but

for NH_3 vibrational energy is almost invariant with both the ligand population and cluster size.

Figure 8 *a* and *b* shows the variation of HOMO–LUMO gap for $\text{Fe}_N(\text{NO})_m$, $\text{Fe}_N(\text{NH}_3)_m$ systems. For all $\text{Fe}_N(\text{NO})_m$ clusters initially the gap increases and then decreases. Though NO is also strong field ligand like CO, we observe different dependence of HOMO–LUMO gap on Fe_N cluster size and ligand population. As more NH_3 molecules are adsorbed on the metal centre, HOMO–LUMO gap for $\text{Fe}_N(\text{NH}_3)_m$ clusters decrease.

Conclusions

Using a pure DFT approach, we have optimized the ground-state geometries of neutral $\text{Fe}_N(\text{CO})_m$ ($N = 1, 4$ and $m = 1, 10$) clusters. The geometric optimization indicates that the ground-state $\text{Fe}_N(\text{CO})_m$ clusters adopt linear structure for $N = 1-2$ and $m = 1-2$. Increasing N and m , we observe different types of three-dimensional structures. Depending on the Fe_N cluster size, CO may be twofold, threefold or fourfold coordinated with the metal centre. Depending on the nature of adsorption (whether terminal or bridging with iron), the Fe–C bond distance varies with the number of CO molecules adsorbed. For strong ligands in the spectrochemical series like NO and CO, the N–O and C–O bond distance and vibrational frequency varies with both Fe_N cluster size and ligand concentration. For weak ligands like NH_3 , there is no effect of cluster size and ligand concentration on N–H bond distance. We also observe from HOMO–LUMO gap that Fe_1CO_5 has the highest chemical stability for $N = 1$. For $m = 2$, $\text{Fe}_2(\text{CO})_4$ has the highest chemical stability. For $N = 3$ and 4, the chemical stability increases with CO adsorption.

1. Heng-Feng, G., Gong-Ping, L. and Yan-Hui, J., Isomers of the Cu_5 cluster: a density function theory study. *Chin. Phys. B*, 2011, **20**, 033105–033110.
2. Zaleski, C. M. *et al.*, Synthesis, structure, and magnetic properties of a large lanthanide transition metal single molecule magnet. *Angew. Chem. Int. Ed. Engl.*, 2004, **30**, 3912–3914.

3. Zeinalipour-Yazdi, C. D., Cooksy, A. L. and Efstathiou, A. M., CO adsorption on transition metal clusters: trends from density functional theory. *Surf. Sci.*, 2008, **602**, 1858–1862.
4. Taylor, K. C., Nitric oxide catalysis in automotive exhaust systems. *Catal. Rev. – Sci. Eng.*, 1993, **35**, 475–481.
5. Nielsen, T. R., Manufacture of hydrogen. *Catal. Today*, 2005, **106**, 293–296.
6. Nikolaev, P., Bronikowski, M. J., Bradely, R. K., Rohmund, F., Colbert, D. T., Smith, K. A. and Smalley, R. E., Gas-phase catalytic growth of single-walled carbon nanotubes from carbon monoxide. *Chem. Phys. Lett.*, 1999, **313**, 313.
7. Castro, M. and Salahub, D. R., Density-functional calculations for small iron clusters: Fe_n , Fe_n^+ , and Fe_n^- for $n \leq 5$. *Phys. Rev. B.*, 1994, **49**, 11842–11852.
8. Jones, N. O., R. B. M., Khanna, S. N., Baruah, T. and Pederson, M. R., Hydrogen adsorption and magnetic behavior of Fe_n and Co_n clusters: controlling the magnetic moment and anisotropy one atom at a time. *Phys. Rev. B*, 2004, **70**, 165406.
9. Griffin, J. B. and Armentrout, P. B., Guided ion-beam studies of the reactions of ($n = 1-8$) with CO_2 : iron cluster oxide bond energies. *J. Chem. Phys.*, 1997, **14**, 5345–5355.
10. Griffin, J. B. and Armentrout, P. B., Guided ion beam studies of the reactions of Fe_n^+ ($n = 2-18$) with O_2 : iron cluster oxide and dioxide bond energies. *J. Chem. Phys.*, 1997, **106**, 4448–4462.
11. Gutsev, G. L. and Buschlicher Jr, C. W., Interaction of carbon atoms with Fe_n , Fe_n^+ and Fe_n^- clusters ($n = 1-6$). *Chem. Phys.*, 2003, **291**, 27–40.
12. Becke, A. D., Density-functional exchange-energy approximation with correct asymptotic behaviour. *Phys. Rev. A*, 1988, **38**, 3098–3100.
13. Lee, C., Yang, W. and Parr, R. G., Development of the Colle–Salvetti correlation-energy formula into a functional of the electron density. *Phys. Rev. B*, 1988, **37**, 785–789.
14. Hay, P. J. and Wadt, W. R., *Ab initio* effective core potentials for molecular calculations. Potentials for the transition metal atoms Sc to Hg. *J. Chem. Phys.*, 1985, **82**, 270–283.
15. Wadt, W. R. and Hay, P. J., *Ab initio* effective core potentials for molecular calculations. Potentials for main group elements Na to Bi. *J. Chem. Phys.*, 1985, **82**, 284–298.
16. Hay, P. J. and Wadt, W. R., *Ab initio* effective core potentials for molecular calculations. Potentials for K to Au including the outermost core orbitals. *J. Chem. Phys.*, 1985, **82**, 299–310.
17. Frisch, M. J. *et al.*, Gaussian 03, Revision C.02, Gaussian, Inc, Wallingford, CT, 2004.
18. Tian, F.-Y., Shen, J. and Wang, Y.-X., Density functional study of CO adsorbed on Mn_N ($N = 2-8$) clusters. *J. Phys. Chem.*, 2010, **114**, 1616–1620.

ACKNOWLEDGEMENT. P.K.G. thanks CSIR, New Delhi for financial support.